

# The Prosurvival IKK-Related Kinase IKK $\epsilon$ Integrates LPS and IL17A Signaling Cascades to Promote Wnt-Dependent Tumor Development in the Intestine

Serkan Ismail Göktuna<sup>1,2,3</sup>, Kateryna Shostak<sup>1,2</sup>, Tieu-Lan Chau<sup>1,2</sup>, Lukas C. Heukamp<sup>4</sup>, Benoit Hennuy<sup>1,5</sup>, Hong-Quan Duong<sup>1,2</sup>, Aurélie Ladang<sup>1,2</sup>, Pierre Close<sup>1,6</sup>, Iva Klevernic<sup>1,2</sup>, Fabrice Olivier<sup>1,7</sup>, Alexandra Florin<sup>4</sup>, Grégory Ehx<sup>1,9</sup>, Frédéric Baron<sup>1,9</sup>, Maud Vandereyken<sup>1,8</sup>, Souad Rahmouni<sup>1,8</sup>, Lars Vereecke<sup>10,11</sup>, Geert van Loo<sup>10,11</sup>, Reinhard Büttner<sup>4</sup>, Florian R. Greten<sup>12</sup>, and Alain Chariot<sup>1,2,13</sup>

## Abstract

Constitutive Wnt signaling promotes intestinal cell proliferation, but signals from the tumor microenvironment are also required to support cancer development. The role that signaling proteins play to establish a tumor microenvironment has not been extensively studied. Therefore, we assessed the role of the proinflammatory Ikk-related kinase Ikk $\epsilon$  in Wnt-driven tumor development. We found that Ikk $\epsilon$  was activated in intestinal tumors forming upon loss of the tumor suppressor *Apc*. Genetic ablation of Ikk $\epsilon$  in  $\beta$ -catenin-driven models of intestinal cancer reduced tumor incidence and consequently extended survival. Mechanistically, we attributed the tumor-promoting effects of Ikk $\epsilon$  to limited TNF-dependent apoptosis in transformed intestinal epithelial cells. In addition, Ikk $\epsilon$  was also required for lipo-

polysaccharide (LPS) and IL17A-induced activation of Akt, Mek1/2, Erk1/2, and Msk1. Accordingly, genes encoding pro-inflammatory cytokines, chemokines, and anti-microbial peptides were downregulated in Ikk $\epsilon$ -deficient tissues, subsequently affecting the recruitment of tumor-associated macrophages and IL17A synthesis. Further studies revealed that IL17A synergized with commensal bacteria to trigger Ikk $\epsilon$  phosphorylation in transformed intestinal epithelial cells, establishing a positive feedback loop to support tumor development. Therefore, TNF, LPS, and IL17A-dependent signaling pathways converge on Ikk $\epsilon$  to promote cell survival and to establish an inflammatory tumor microenvironment in the intestine upon constitutive Wnt activation. *Cancer Res*; 76(9); 2587–99. ©2016 AACR.

<sup>1</sup>Interdisciplinary Cluster for Applied Genoproteomics (GIGA), University of Liege, Liège, Belgium. <sup>2</sup>Laboratory of Medical Chemistry, GIGA Molecular Biology of Diseases, University of Liege, Liège, Belgium. <sup>3</sup>Department of Molecular Biology and Genetics, Bilkent University, Bilkent, Ankara, Turkey. <sup>4</sup>Institute for Pathology-University Hospital Cologne, Germany. <sup>5</sup>GIGA Transcriptomic Facility, University of Liege, CHU, Sart-Tilman, Liège, Belgium. <sup>6</sup>Laboratory of Cancer Signaling, GIGA Molecular Biology of Diseases, University of Liege, Liège, Belgium. <sup>7</sup>Animal Facility, Liège, University of Liege, Belgium. <sup>8</sup>Unit of Immunology and Infectious Diseases, GIGA Molecular Biology of Diseases, University of Liege, Liège, Belgium. <sup>9</sup>Unit of Hematology and Department of Medicine, Division of Hematology, GIGA-I<sup>3</sup>, University of Liege, Liège, Belgium. <sup>10</sup>Inflammation Research Centre (IRC), VIB, Ghent, Belgium. <sup>11</sup>Department of Biomedical Molecular Biology, Ghent University, Ghent, Belgium. <sup>12</sup>Georg-Speyer-Haus, Institute for Tumor Biology and Experimental Therapy, 60596 Frankfurt am Main, Germany. <sup>13</sup>Walloon Excellence in Life Sciences and Biotechnology (WELBIO), University of Liege, Liège, Belgium.

**Note:** Supplementary data for this article are available at Cancer Research Online (<http://cancerres.aacrjournals.org/>).

S.I. Göktuna and K. Shostak contributed equally to this article.

**Corresponding Author:** Alain Chariot, GIGA Molecular Biology of Diseases, University of Liege, Avenue de l'Hôpital, 1, CHU, Sart-Tilman, Liège 4000, Belgium. Phone: 32-4-366-24-72; Fax: 32-4-366-45-34; E-mail: [alain.chariot@ulg.ac.be](mailto:alain.chariot@ulg.ac.be)

**doi:** 10.1158/0008-5472.CAN-15-1473

©2016 American Association for Cancer Research.

## Introduction

Colorectal cancer results from multiple genetic mutations and inflammatory processes (1). Somatic mutations associated with 80% of colorectal cancer cases target the adenomatous polyposis coli (*APC*) tumor suppressor gene, which leads to  $\beta$ -catenin activation, followed by additional mutations in *K-Ras*, *PI3K3CA*, and *TP53* among others as tumors develop (2, 3).

The majority of colorectal cancer cases have no preexisting inflammation but nevertheless displays tissue infiltration by inflammatory cells, which is referred to as "tumor-elicited inflammation" (4, 5). Those infiltrates include CD4<sup>+</sup> T-helper 1 (Th1) and CD8<sup>+</sup> cytotoxic T cells (CTL), tumor-associated macrophages (TAM), and T-helper interleukin 17 (IL17)-producing (Th17) cells. The tumor-promoting functions of TAMs and T lymphocytes are mediated through the secretion of cytokines. TAMs produce IL23, which enhances tumor-promoting inflammatory processes through IL17A synthesis by Th17 cells and also suppresses the adaptive immune surveillance by reducing CD8<sup>+</sup> CTL cell infiltration in tumors (4, 6–8). In turn, IL17A triggers MAPKs and NF- $\kappa$ B activations in intestinal epithelial cells (IEC) to support early tumor growth (9).

The establishment of a tumor microenvironment relies on transcription factors such as NF- $\kappa$ B (10, 11). I $\kappa$ B-kinase (Ikk)  $\beta$ -dependent NF- $\kappa$ B activity in IECs promotes cell survival and

drives the expression of proinflammatory cytokines in myeloid cells to link inflammation to cancer (12). In addition, NF- $\kappa$ B signaling in IECs also cooperates with  $\beta$ -catenin to facilitate the crypt stem cell expansion (13).

Both NF- $\kappa$ B and Stat3 transcription factors are activated by cytokines through parallel signaling pathways in solid tumors (14). Similar to NF- $\kappa$ B, Stat3 controls the expression of genes involved in cell survival, proliferation, and immunity. IL6, whose expression relies on NF- $\kappa$ B in lamina propria myeloid cells, protects premalignant IECs from apoptosis through Stat3 activation in a model of colitis-associated cancer (15, 16). IL23 signaling also promotes Stat3 phosphorylation in *Apc*-mutated IECs through IL17A production by Th17 cells (7).

Constitutive  $\beta$ -catenin activation and/or *Apc* loss in the intestinal epithelium cause the loss of epithelial barrier function, an early event in intestinal tumorigenesis (7). As a result, commensal bacteria infiltrate the stroma and lead to tumor-associated inflammation (17). Bacterial products are sensed by Toll-like receptors (TLR) such as TLR4, which promotes colitis-associated cancer (18).

TLR signaling triggers IKK $\beta$ /NF- $\kappa$ B activation, leading to synthesis of proinflammatory cytokines and the phosphorylation of IKK-related kinases TBK1 and IKK $\epsilon$  to induce type I interferons synthesis through IRF3 (19–21). IKK $\epsilon$  is believed to play key roles in cancer by targeting multiple substrates, many of which act in NF- $\kappa$ B-dependent pathways (22–25). Both TBK1 and IKK $\epsilon$  also directly phosphorylate AKT/protein kinase B (26, 27). So far, it remains to be demonstrated that IKK $\epsilon$  acts as an oncogenic kinase *in vivo*.

Here we report that LPS and IL17A-dependent signaling pathways converge to Ikke to promote Wnt-dependent tumor development in IECs *in vivo*. These pathways drive the expression of proinflammatory cytokines, anti-microbial peptides, and chemokines, the latter recruiting macrophages to support IL23 and IL17A synthesis and subsequent Stat3 activation in transformed IECs. Ikke also promotes cell survival in these cells by limiting TNF- and caspase-8-dependent apoptosis. The establishment of an inflammatory tumor-promoting microenvironment by Ikke thus relies on the activation of signaling pathways distinct from the NF- $\kappa$ B-dependent cascades.

## Materials and Methods

### Mouse models

*Villin-Cre-ER<sup>T2</sup> Ctnnb1<sup>+lox(ex3)</sup> ( $\beta$ -cat<sup>c.a.</sup>)* mice were previously described (28, 29). *Villin-Cre-ER<sup>T2</sup> Ctnnb1<sup>+lox(ex3)</sup>* mice were gavaged 5 consecutive days with 1 mg tamoxifen (Sigma) to induce  $\beta$ -catenin activation in enterocytes as described previously (30). Both *Apc<sup>+min</sup>* and *Ikke<sup>KO</sup>* mouse strains were from Jackson Laboratories (Bar Harbor, ME). For antibiotics treatments, 0.5 g ciprofloxacin, 1 g ampicillin, and 0.5 g metronidazole per liter were added in the drinking water 1 week before tamoxifen administration. All mice used were 8 to 16 weeks old when started with experiments (except for the *Apc<sup>+min</sup>* survival experiments) and littermate controls were used. All procedures were approved by the local Ethical Committee of the University of Liege.

### Bone marrow transplantation

Bone marrow transplantation and bone marrow cell isolation were done as described previously (30). Minor changes are described in the Supplementary data section.

### Ex vivo organoid cultures

Intestinal crypts from *Apc<sup>+min</sup> Ikke<sup>-/-</sup>* and *Apc<sup>+min</sup> Ikke<sup>+/+</sup>* mice were isolated and cultured as described (31). Stimulations of *ex vivo* organoid cultures with IL17A and LPS were carried out as described (9).

### Determination of proliferation and apoptosis

Mice were injected intraperitoneal with 100 mg/kg BrdU (Sigma) 90 minutes before their sacrifice and paraffin sections of duodenum tissues were stained using anti-BrdU antibody (RPN201; Amersham Biosciences/GE Healthcare) to quantify proliferating nuclei. Proliferative rates were determined by the ratio of average of positive cells in 10 crypts or by the ratio of positive cells to total cells in three proliferative cryptic area (where individual crypts could no longer be identified) per sample. Apoptotic cells in a given tissue section were determined histologically by TUNEL assay using an ApoAlert DNA Fragmentation Assay Kit (BD Biosciences Clontech).

### Cell culture

SW480, HCT116, and HT-29 cells were obtained from ATCC in 2009. These cells were characterized by ATCC, using a comprehensive database of short tandem repeat (STR) DNA profiles. Frozen aliquots of freshly cultured cells were generated and experiments were done with resuscitated cells cultured for less than 6 months. Cell culture reagents, cytokines, and kinase inhibitors are described in the Supplementary data.

### Lentiviral cell infection

Infections of Lenti-X 293T cells (Clontech) using lentiviral constructs described in the Supplementary data were carried out as previously described (32).

### Protein expression, histological analysis, and immunoprecipitations

Isolation of enterocytes and Western blot analyses were performed as described previously (30). Paraffin sections (4  $\mu$ m) and Western blots were stained using antibodies described in the Supplementary data section. For Immunoprecipitations, anti-TANK, -NAP1 and -IgG (negative control) antibodies were coupled covalently to a mixture of Protein A/G-Sepharose (see the Supplementary data for details). Immunoprecipitations were done as previously described (33).

### Quantitative real-time PCR and RNA-seq expression analyses

Total RNAs were extracted and subjected to real-time PCR analyses as described (32). Primer sequences are available on request. Gene expression profiling of tumor tissues was carried out by RNA-Seq analysis. Both sample preparations and sequencing were performed at the GIGA transcriptomic facility (GIGA, University of Liege, Liege, Belgium). Methods to check total RNAs integrity, to carry out RNA-Seq expression analyses and for data analysis are described in the Supplementary Data.

### In situ hybridization

Sample tissues were fixed with the standard procedures using 4% PFA (1 hour) and sucrose (15% 6 hours; 30% o/n) at 4°C and frozen in OCT freezing medium by the use of supercooled isopropanol-dry ice mixture and stored at -80°C up to 6 month.

Frozen samples were cut 5 to 10  $\mu\text{m}$  with a cryostat microtome at  $-20^{\circ}\text{C}$  on superfrost slides. *In situ* hybridization was carried out using the protocol provided by the manufacturer (RNAscope Multiplex Assay System; Advanced Cell Diagnostics Inc.).

#### FACS analyses

Control or IKK $\epsilon$ -depleted SW480 cells were pretreated or not with the pan-caspase inhibitor Z-VAD-FMK (Promega; 20  $\mu\text{mol/L}$ ) for 1 hour and subsequently untreated or stimulated with TNF (100 ng/mL)/cycloheximide (CHX; 50  $\mu\text{g/mL}$ ) for up to 8 hours. The quantification of apoptosis was done as previously described (32).

#### Statistical analysis

Data are expressed as mean  $\pm$  SEM. Differences were analyzed by Student *t*-test or log-rank test (for Kaplan–Meier survival graphs of animal models) using Prism5 (GraphPad Software). The *P* values  $\leq 0.05$  (covering 95% confidence intervals) were considered significant (30).

## Results

### Wnt-driven tumor development in the intestine relies on Ikke

We investigated whether *Ikke* inactivation impacts on tumor formation in the *Apc*<sup>+/*min*</sup> mouse model, which spontaneously develops adenocarcinomas due to constitutive Wnt signaling (34). Inactivating *Ikke* in *Apc*<sup>+/*min*</sup> mice significantly enhanced survival (226 days vs. 143 days, *P* < 0.001 in *Apc*<sup>+/*min*</sup>-*Ikke*<sup>-/-</sup> and *Apc*<sup>+/*min*</sup>-*Ikke*<sup>+/+</sup> mice, respectively) due to a decreased tumor incidence in distinct parts of the intestine (Fig. 1A–D). As a result, *Apc*<sup>+/*min*</sup>-*Ikke*<sup>-/-</sup> mice did not suffer from anemia and splenomegaly was less dramatic (Fig. 1E and F, respectively). *Ikke* deletion slightly impaired cell proliferation in tumors but not in normal intestinal crypts in *Apc*<sup>+/*min*</sup> mice (Fig. 1G). Consistently, pErk1/2 levels and, to some extent, cell proliferation as assessed by BrdU staining, were decreased in *Apc*<sup>+/*min*</sup>-*Ikke*<sup>-/-</sup> mice (Fig. 1H). *Ikke* did not control cell proliferation in a cell-autonomous manner as *ex vivo* organoids generated with intestinal crypts from *Apc*<sup>+/*min*</sup>-*Ikke*<sup>-/-</sup> and *Apc*<sup>+/*min*</sup>-*Ikke*<sup>+/+</sup> mice showed similar cell growth (Supplementary Fig. S1A). *Ikke* phosphorylation on serine 172 was higher in intestinal tumors than in normal adjacent tissues from *Apc*<sup>+/*min*</sup> mice, as were protein levels of Tank, one of the *Ikke* scaffold proteins (Supplementary Fig. S1B).

We took advantage of the tamoxifen-inducible  $\beta$ -cat<sup>c.a.</sup> mouse model, which expresses truncated and stabilized  $\beta$ -catenin protein in IECs (28). Intestinal crypts rapidly expand because of constitutive Wnt signaling and loss of differentiated IECs, with  $\beta$ -cat<sup>c.a.</sup> mice succumbing to disease within 4 weeks of age because of continuous adenoma formation (13). *Ikke* mRNA expression was detected by *in situ* hybridization both in transformed IECs and in inflammatory cells (Fig. 2A). *Ikke* inactivation in  $\beta$ -cat<sup>c.a.</sup> mice also extended their survival (37 vs. 30 and 28.5 days, *P* = 0.0044 in  $\beta$ -cat<sup>c.a.</sup>-*Ikke*<sup>-/-</sup>,  $\beta$ -cat<sup>c.a.</sup>-*Ikke*<sup>+/-</sup>, and  $\beta$ -cat<sup>c.a.</sup>-*Ikke*<sup>+/+</sup> mice, respectively; Fig. 2B). *Ikke* was essential for Akt, Mek1/2, Erk1/2, and Msk1 activation and for Creb1 (a Msk1 substrate) and Stat3 phosphorylation but not for Wnt-dependent Pdk1 phosphorylation (Fig. 2C and Supplementary Fig. S2, respectively). Tank expression was also higher upon constitutive Wnt signaling (Fig. 2C). Enhanced pAkt and pErk1/2 levels in tumors from  $\beta$ -cat<sup>c.a.</sup>-*Ikke*<sup>+/+</sup> versus  $\beta$ -cat<sup>c.a.</sup>-*Ikke*<sup>-/-</sup> mice were confirmed by Immunohistochemistry (Fig. 2D). Thus, *Ikke* promotes the

activation of multiple oncogenic pathways in transformed IECs to support tumor development.

### Ikke protects from TNF-dependent cell apoptosis in transformed intestinal epithelial cells

As Wnt-driven tumor development was impaired upon *Ikke* deficiency, we next explored whether this resulted from enhanced cell death. *Ikke* inactivation in *Apc*<sup>+/*min*</sup> mice enhanced the number of TUNEL<sup>+</sup> cells in small intestinal tumors (Fig. 3A). Consistently, IKK $\epsilon$ -deficient and p53-mutated colon cancer SW480 cells were sensitized to TNF + CHX-dependent cell death, as judged by FACS analysis (Fig. 3B). IKK $\epsilon$ -deficient SW480 cells were dying of apoptosis as the caspase inhibitor Z-VAD-FMK blocked TNF/CHX-dependent cell death (Fig. 3B). Consistently, IKK $\epsilon$ -deficient SW480 cells subjected to TNF/CHX stimulation showed increased levels of cleaved forms of caspases 3/8 and RIPK1, a caspase-8 substrate (Fig. 3C). Cell death in IKK $\epsilon$ -deficient SW480 cells did not result from decreased NF- $\kappa$ B activity as the TNF-dependent I $\kappa$ B $\alpha$  degradation and p65 phosphorylation were unchanged (Supplementary Fig. S3). The TNF-dependent activation of the other IKK-related kinase TBK1 was potentiated upon IKK $\epsilon$  deficiency, suggesting a compensatory mechanism (Supplementary Fig. S3). Enhanced cell apoptosis was also seen upon TNF/CHX stimulation in other IKK $\epsilon$ -deficient colon cancer cell lines showing constitutive Wnt signaling, namely in p53-mutated HT29 and in p53-proficient HCT116 cells (Supplementary Fig. S4A–S4C). Therefore, IKK $\epsilon$  protects from TNF-dependent apoptosis through p53- and NF- $\kappa$ B-independent mechanisms in transformed IECs.

### LPS- and IL17A-dependent pathways converge to IKK $\epsilon$ in colon cancer-derived cell lines

We next characterized the IKK $\epsilon$ -dependent pathways in colon cancer cells. Constitutive phosphorylation of ERK1/2 relied on IKK $\epsilon$  in differentiated HT-29 cells (Supplementary Fig. S5A). Moreover, Lipopolysaccharide (LPS)-induced phosphorylation of ERK1/2 was defective in IKK $\epsilon$ -depleted SW480 cells (Supplementary Fig. S5B). Thus, our data link IKK $\epsilon$  to ERK1/2 activation in transformed IECs.

IL17A signals in transformed IECs and IKK $\epsilon$  is activated by IL-17A in airway epithelial cells (9, 35, 36). Therefore, we assessed if IL17A promotes Wnt-dependent tumor development through IKK $\epsilon$ . IL-17A alone or in combination with LPS triggered IKK $\epsilon$  phosphorylation in *ex-vivo* organoid cultures of transformed IECs (Supplementary Figs. S6A and 4A, respectively). IKK $\epsilon$  deficiency in *ex-vivo* organoid cultures from *Apc*<sup>+/*min*</sup> mice as well as in SW480 cells impaired AKT, MEK1, p38 and ERK1/2 activation upon stimulation with both LPS and IL17A (Fig. 4A and B, respectively). IKK $\epsilon$  constitutively bound TANK but not with NAP1, another scaffold protein, in unstimulated or IL17A-treated SW480 cells (Supplementary Fig. S6B). TANK deficiency also severely impaired AKT, MEK1/2, ERK1/2 and p38 activation in cells stimulated with both LPS and IL17A (Supplementary Fig. S7). Therefore, the IKK $\epsilon$ -TANK complex integrates LPS- and IL17A-dependent cascades to activate multiple kinases.

### Ikke establishes a proinflammatory signature in the intestine upon constitutive Wnt signaling

To identify target genes induced through *Ikke*, RNA-Seq analysis was done using total RNAs from duodenal samples of

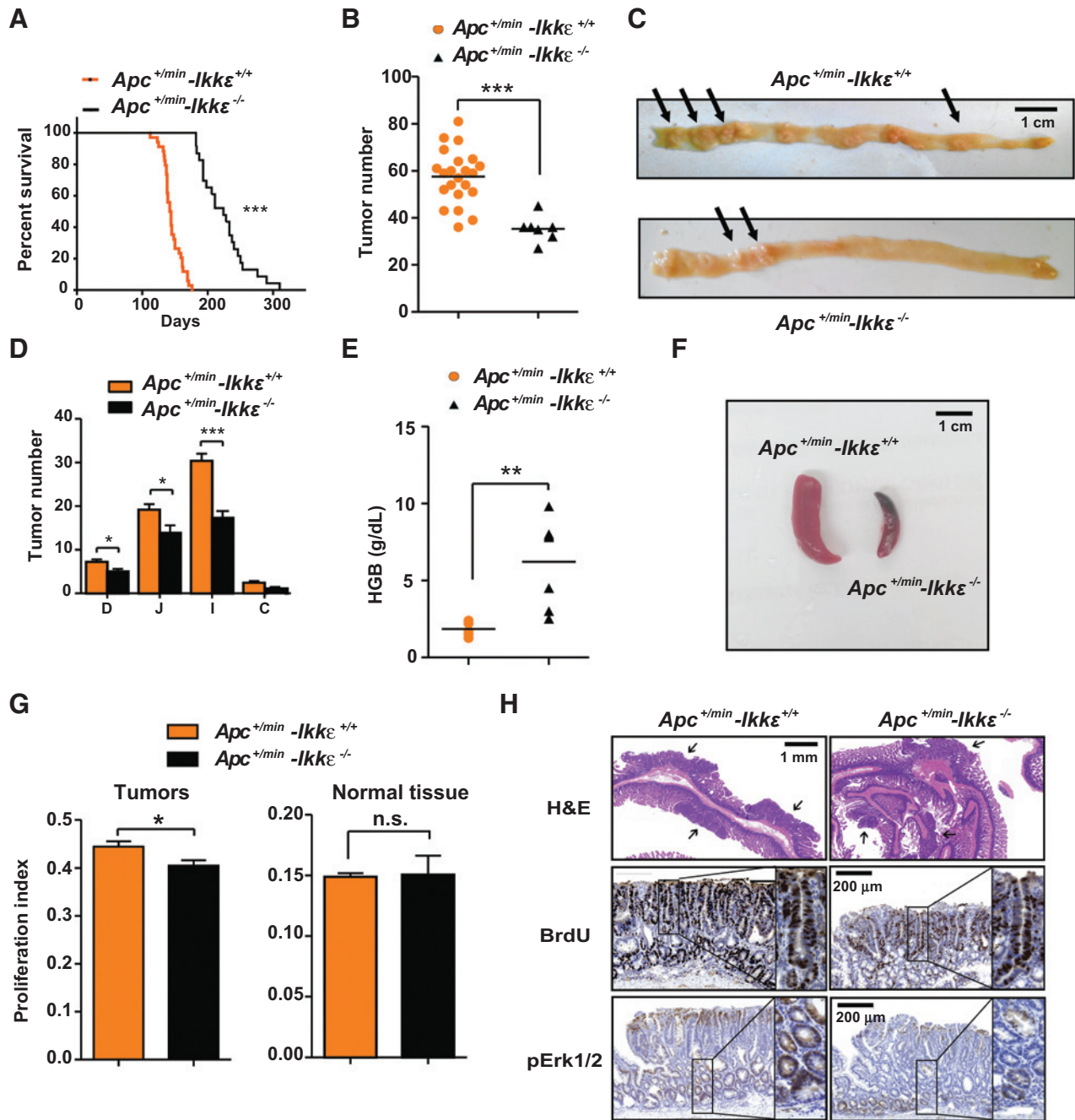
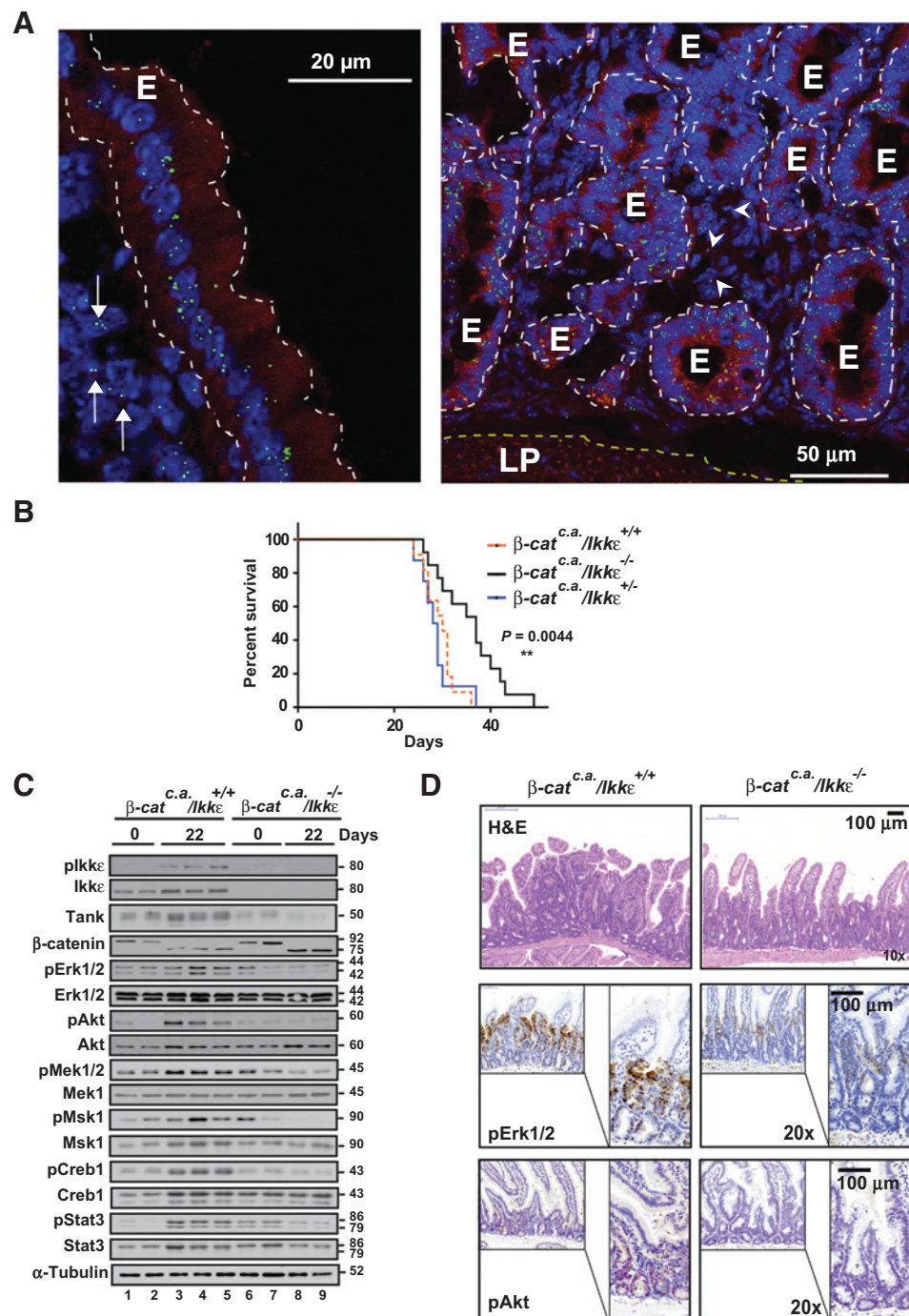


**Figure 1.** Loss of *Ikke* impairs tumor development in *Apc<sup>+ / min</sup>* mice. A, extended survival upon *Ikke* deficiency in the *Apc<sup>+ / min</sup>* model. A, Kaplan–Meier survival graph is shown for *Apc<sup>+ / min</sup>Ikke<sup>+ / +</sup>* ( $n = 34$ ) and *Apc<sup>+ / min</sup>Ikke<sup>- / -</sup>* ( $n = 15$ ) mice (\*\*\*,  $P < 0.001$ ; log-rank test). B, decreased tumor incidence in 4 months old *Apc<sup>+ / min</sup>Ikke<sup>- / -</sup>* ( $n = 7$ ) versus *Apc<sup>+ / min</sup>Ikke<sup>+ / +</sup>* ( $n = 19$ ) mice. Data are mean  $\pm$  SEM (\*\*\*,  $P < 0.001$ ; Student *t* test). C, representative pictures of duodenum from 4 months old *Apc<sup>+ / min</sup>Ikke<sup>+ / +</sup>* and *Apc<sup>+ / min</sup>Ikke<sup>- / -</sup>* mice. D, *Ikke* deficiency impairs tumor development. Distribution of intestinal tumors in 4 months old mice of the indicated genotype (D, duodenum; J, jejunum; I, ileum; C, colon). Data are mean  $\pm$  SEM,  $n \geq 7$  for each genotype (\*,  $P < 0.05$  and \*\*\*,  $P < 0.001$ ; Student *t* test). E, *Ikke* deficiency reduces anemia in *Apc<sup>+ / min</sup>* mice. Blood hemoglobin (HGB) levels in 4 months old mice of the indicated genotype were quantified. Data are mean  $\pm$  SE,  $n \geq 5$  for each genotype (\*\*,  $P < 0.01$ ; Student *t* test). F, *Ikke* deficiency limits splenomegaly in *Apc<sup>+ / min</sup>* mice. Representative pictures of the spleen from 4 months old mice of the indicated genotype. G, *Ikke* deficiency impacts on cell proliferation in tumors but not in normal crypts in the *Apc<sup>+ / min</sup>* model. The BrdU proliferation index in tumors and normal crypts of 4 months old *Apc<sup>+ / min</sup>Ikke<sup>+ / +</sup>* and *Apc<sup>+ / min</sup>Ikke<sup>- / -</sup>* mouse tumors is shown (left and right, respectively). Data are mean  $\pm$  SEM,  $n \geq 3$  for each genotype (\*,  $P < 0.05$ ; Student *t* test). n.s., nonsignificant. H, *Ikke* promotes Erk1/2 activation in the *Apc<sup>+ / min</sup>* model. H&E staining, BrdU, and pErk1/2 immunohistological analyses of tumors of mice of the indicated genotype are shown.

**Figure 2.**

*Ikke* promotes tumor development in the  $\beta$ -cat<sup>c.a.</sup> tumor initiation model through Akt, Mek1, and Erk1/2 activations. A, *Ikke* expression in IECs in the  $\beta$ -cat<sup>c.a.</sup> model. *In situ* hybridization for *Ikke* mRNA in duodenal highly proliferating cryptic sections from  $\beta$ -cat<sup>c.a.</sup> mice, 22 days after first tamoxifen injection [green channel is for sample probe (*Ikke*), red channel is for negative control probe (DapB), and blue channel is for DAPI]. Single dot signals are seen in *Ikke*-expressing epithelial (E) cells and, to a lesser extent, in inflammatory cells (arrows). LP, lamina propria. B, extended survival upon *Ikke* deficiency in the  $\beta$ -cat<sup>c.a.</sup> model. A, Kaplan–Meier survival graph for  $\beta$ -cat<sup>c.a.</sup>/*Ikke*<sup>+/+</sup> (*n* = 7),  $\beta$ -cat<sup>c.a.</sup>/*Ikke*<sup>+/-</sup> (*n* = 7),  $\beta$ -cat<sup>c.a.</sup>/*Ikke*<sup>-/-</sup> (*n* = 13) mice after induction of tumorigenesis via 5 days tamoxifen injections is illustrated (\*, *P* < 0.05; log-rank test). Data are mean  $\pm$  SEM, *n*  $\geq$  5 for each genotype. C, impaired activation of multiple pathways upon *Ikke* deficiency in the  $\beta$ -cat<sup>c.a.</sup> model. Extracts of duodenal epithelium from  $\beta$ -cat<sup>c.a.</sup>/*Ikke*<sup>+/+</sup> and  $\beta$ -cat<sup>c.a.</sup>/*Ikke*<sup>-/-</sup> mice, 0 and 22 days after the first tamoxifen injection were subjected to Western blotting using the indicated antibodies. D, impaired Erk1/2 activations upon *Ikke* deficiency in the  $\beta$ -cat<sup>c.a.</sup> model. H&E and BrdU stainings and T202/Y204 pErk1/2 and S473 pAkt IHC analysis of duodenal epithelium from the indicated mice, 22 days after the first tamoxifen injection are showed.



$\beta$ -cat<sup>c.a.</sup>-*Ikke*<sup>+/+</sup> and  $\beta$ -cat<sup>c.a.</sup>-*Ikke*<sup>-/-</sup> mice, 0 and 22 days following tamoxifen administration and WebGestalt GSAT enrichment analysis was carried out. A remarkable number of *Ikke*-regulated genes were involved in the immune response (Supplementary Figs. S8A and S8B). GSEA analysis further highlighted defective interferon and innate immune responses in  $\beta$ -cat<sup>c.a.</sup>-*Ikke*<sup>-/-</sup> mice 22 days after tamoxifen administration (Fig. 5A). Consistently, a heatmap representation of gene expression demonstrated the lack of upregulation of immune response genes in duodenal extracts

from  $\beta$ -cat<sup>c.a.</sup>-*Ikke*<sup>-/-</sup> mice compared to  $\beta$ -cat<sup>c.a.</sup>-*Ikke*<sup>+/+</sup> mice (Fig. 5A). These candidates included Fcμr (Fc receptor, IgA, IgM, high affinity), Aicda (Activation-induced cytidine deaminase), Fcrl5 (Fc Receptor-like 5), Reg3β/γ (regenerating islet-derived protein 3-beta/gamma), IL23A, and IL17A (Fig. 5A). Among the 236 downregulated transcripts in  $\beta$ -cat<sup>c.a.</sup>-*Ikke*<sup>-/-</sup> tissue, many were proinflammatory genes (Supplementary Fig. S9A). The most prominent candidates were *Ly6a/c*, *Retnlb*, *Cxcl9*, *C3*, and *Nlrp5* (Supplementary Fig. S9A). In addition, RNA-Seq data revealed

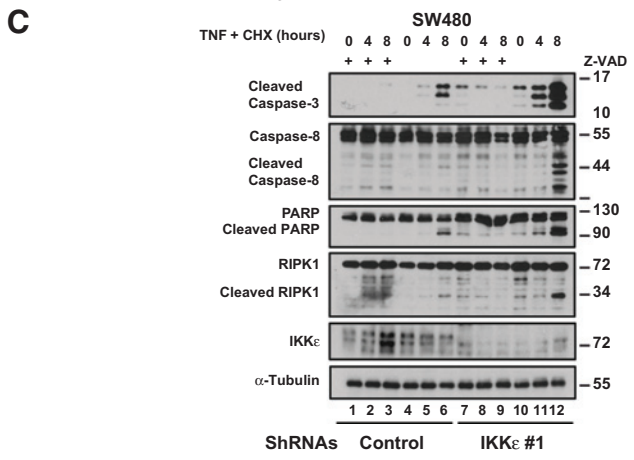
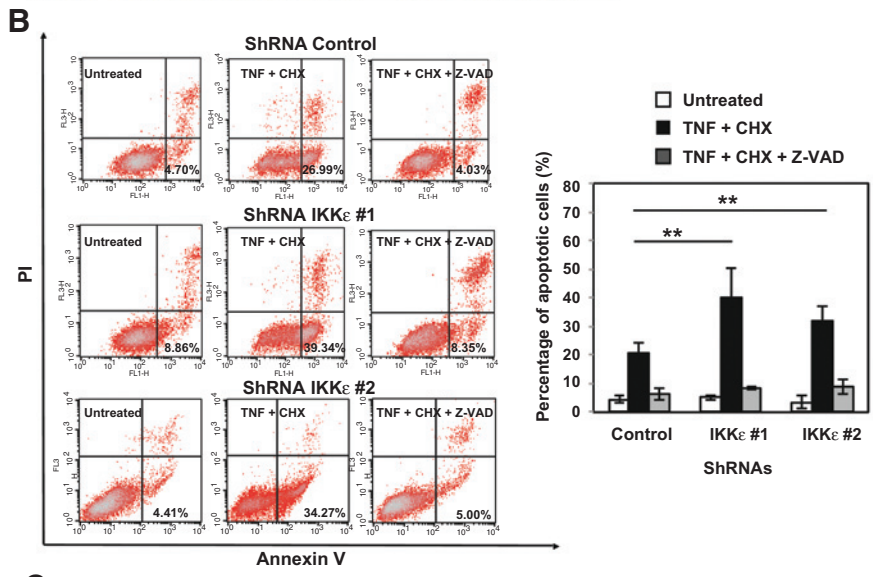
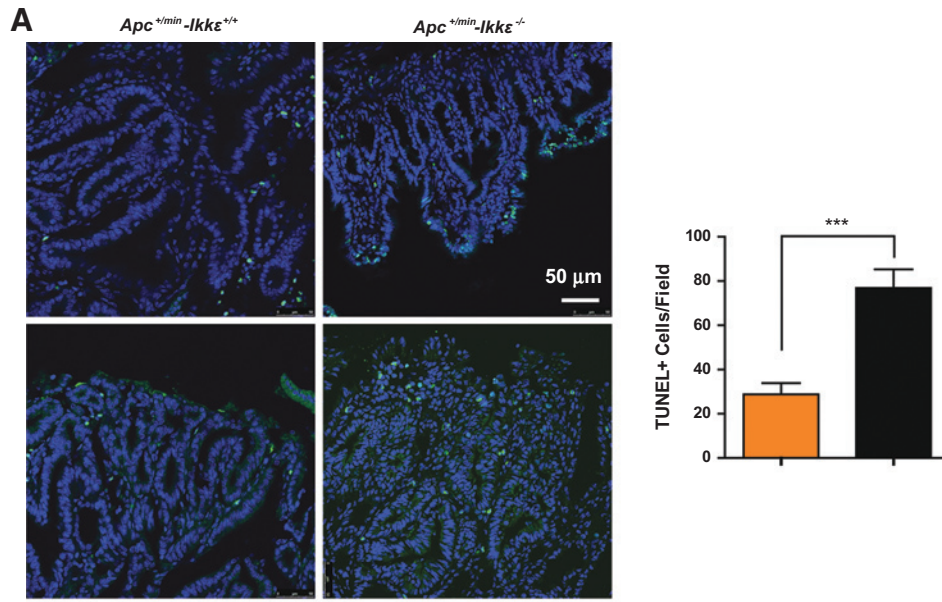


**Figure 3.** Ikkε protects from TNF-dependent cell death in transformed intestinal epithelial cells. A, Ikkε expression protects from cell death *in vivo*. TUNEL stainings (left) and cell death index as quantified by the number of TUNEL<sup>+</sup> cells per field (right) of 4 months old *Apc<sup>+min</sup>/Ikkε<sup>+/+</sup>* or *Apc<sup>+min</sup>/Ikkε<sup>-/-</sup>* small intestinal tumors. \*\*\*, *P* < 0.001 by Student *t* test, *n* ≥ 2 per genotype. B, IKKε protects from TNF/CHX-dependent apoptosis in colon cancer cells. Control or IKKε-deficient SW480 cells were pretreated or not with Z-VAD-FMK (20 μmol/L) for 1 hour, followed by a treatment with TNF (100 ng/mL) and CHX (50 μg/mL). FACS analyses were done to quantify apoptotic cells. The histogram shows FACS data from three independent experiments (Student *t* test; \*\*, *P* < 0.01). C, IKKε deficiency enhances caspase-3/8 activation upon stimulation with TNF and CHX in colon cancer cells. Control or IKKε-depleted SW480 cells were treated with TNF (100 ng/mL) and CHX (50 μg/mL) and cell extracts were subjected to Western blotting.

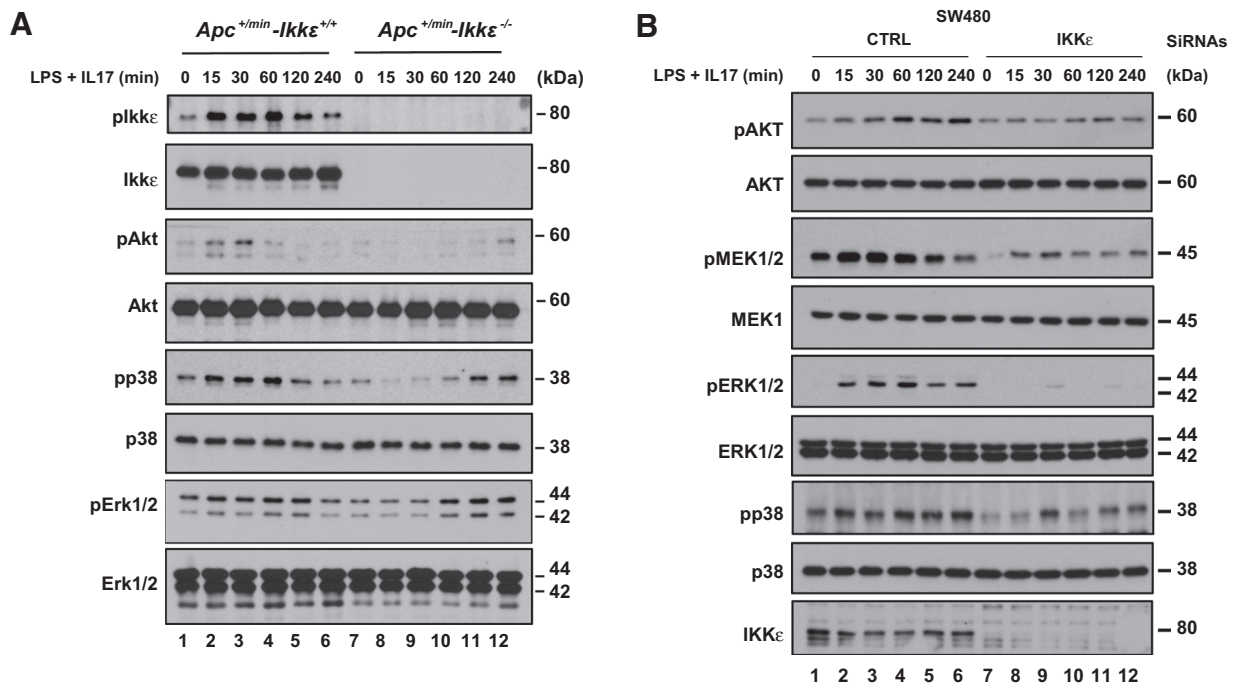


**Figure 4.**

Impaired activation of multiple oncogenic pathways upon *Ikke* deficiency in transformed intestinal epithelial cells. A and B, *Ikke* promotes Akt, p38, and Erk1/2 activation upon stimulation with both LPS and IL17A in IECs showing constitutive Wnt signaling. *Ex vivo* organoid cultures from *Apc<sup>+/min</sup>Ikke<sup>+/+</sup>* and *Apc<sup>+/min</sup>Ikke<sup>-/-</sup>* mice (A) or control and IKKε-depleted SW480 cells (B) were treated or not with both LPS (1 ng/ml) and IL17A (50 ng/ml). Cell extracts were subjected to Western blotting.

numerous chemokines whose expression required *Ikke* upon constitutive Wnt activation in the intestine. Indeed, mRNA levels of *Cxcl12* (also referred as to SDF-1 $\alpha$ ), *Cxcl5*, and *Cxcl1* were severely downregulated upon *Ikke* inactivation (Fig. 5B). A chemokine/cytokine protein array confirmed the decreased expression of chemokines, including *Cxcl9*, *Cxcl11*, *Cxcl12*, *G-Csf*, and cytokines (IL7 and IL17A) in whole duodenal extracts from  *$\beta$ -cat<sup>c.a.</sup>-Ikke<sup>-/-</sup>* mice (Fig. 5C). In contrast, *IL1 $\alpha$*  was upregulated in these conditions (Fig. 5C). *Ikke* deficiency impairs Stat3 phosphorylation in transformed IECs (Fig. 2C), possibly because of an impaired IL17A production rather than from an intrinsic signaling defect. IL17A controls STAT3 phosphorylation through IL6. IKKε was dispensable for IL6-dependent STAT3 activation in SW480 cells, which demonstrates that *Ikke* controls Stat3 phosphorylation through a paracrine mechanism involving IL17A production in  *$\beta$ -cat<sup>c.a.</sup>* mice (Supplementary Fig. S9B).

IL17A synergizes with TNF to induce *Cxcl1* expression through IKKε in airway epithelial cells (36). The combination of LPS and IL17A failed to induce *Cxcl1* expression in both *ex vivo* organoid cultures from *Apc<sup>+/min</sup>-Ikke<sup>-/-</sup>* mice and in IKKε-depleted SW480 cells, as was the induction of *Cxcl1* expression by LPS or IL17A alone (Fig. 5D and Supplementary Fig. S9C, respectively). Therefore, LPS and IL17 signals converge to IKKε to induce *Cxcl1* expression in transformed IECs. AKT or ERK1/2 inhibitors (perifosine, GSK690693, and PD98059, respectively) interfered with the induction of *Cxcl1* expression (Supplementary Fig. S9D). Therefore, IL17A and LPS signal through both AKT and ERK1/2 to induce *Cxcl1* expression in colon cancer cells.

#### Cell autonomous IKKε-dependent expression of inflammatory markers in IECs triggers the recruitment of macrophages to the tumor stroma

Consistent with a role of *Ikke* in chemokines production, the number of macrophages infiltrating the tumor stroma of  *$\beta$ -cat<sup>c.a.</sup>/Ikke<sup>-/-</sup>* mice was significantly decreased, as evidenced by anti-F4/80 and CD163 immunofluorescence (IF) analysis (Fig. 5E and F). Reduced expression of both F4/80 and CD163 upon *Ikke* deficiency was also revealed through real-time PCR analysis (Fig. 5G). Yet, *Ikke* deletion did not impact on macrophages polarization as both M1 and M2 markers were similarly downregulated in duodena of  *$\beta$ -cat<sup>c.a.</sup>/Ikke<sup>-/-</sup>* mice (Fig. 5H). *Cd4*, *Cd8a*, and *Cd68* mRNA levels were also downregulated in these samples (Fig. 5G). Therefore, *Ikke* in IECs promotes the recruitment of macrophages to the tumor stroma through the expression of macrophage-attracting chemokines.

To assess whether *Ikke* expression in hematopoietic cells also contributed to intestinal tumor development, bone marrow cells from  *$\beta$ -cat<sup>c.a.</sup>-Ikke<sup>+/+</sup>* or  *$\beta$ -cat<sup>c.a.</sup>-Ikke<sup>-/-</sup>* mice were isolated and transplanted intravenously to irradiated  *$\beta$ -cat<sup>c.a.</sup>-Ikke<sup>-/-</sup>* or  *$\beta$ -cat<sup>c.a.</sup>-Ikke<sup>+/+</sup>* mice. Mice were kept for a month for the regeneration of immune cells before tamoxifen administration (Supplementary Fig. S10). Irradiated  *$\beta$ -cat<sup>c.a.</sup>-Ikke<sup>-/-</sup>* mice transplanted with bone marrow from *Ikke<sup>-/-</sup>* mice survived longer than  *$\beta$ -cat<sup>c.a.</sup>-Ikke<sup>+/+</sup>* mice transplanted with bone marrow from *Ikke<sup>+/+</sup>* mice (33.5 days versus 27 days, respectively), which confirms the contribution of IKKε in Wnt-driven tumor development (Supplementary Fig. S10).  *$\beta$ -cat<sup>c.a.</sup>-Ikke<sup>+/+</sup>* mice transplanted with bone marrow from *Ikke<sup>-/-</sup>* mice also survived longer (34.6 days), suggesting a contribution of *Ikke* expression in

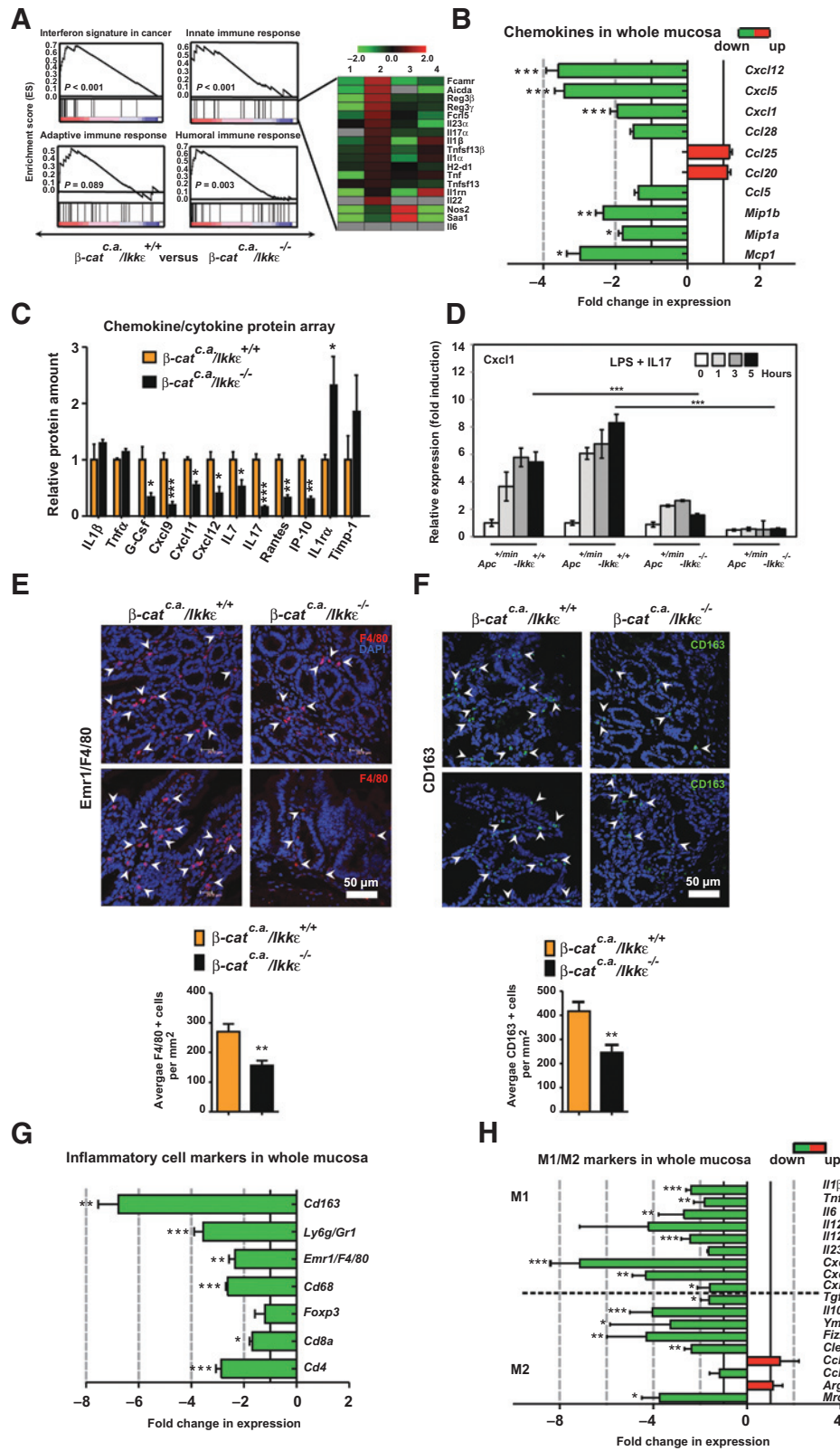


**Figure 5.** Ikkε controls intestinal proinflammatory gene expression and myeloid cell infiltration upon constitutive Wnt signaling. A, defective interferon signature and immune response upon Ikkε deficiency in  $\beta$ -cat<sup>c.a.</sup> mice. A, gene set enrichment analysis of RNA-Seq expression data obtained with total RNAs from duodenal samples of the indicated mice is illustrated. Right, heatmap expression analysis from RNAseq data. (Continued on the following page.)

hematopoietic cells in the observed phenotype. Yet, irradiated  $\beta\text{-cat}^{c.a.}\text{-Ikke}^{-/-}$  mice transplanted with bone marrow from  $\text{Ikke}^{-/-}$  or  $\text{Ikke}^{+/+}$  mice also showed a similar survival advantage (34 and 33.5 days, respectively) compared to irradiated  $\beta\text{-cat}^{c.a.}\text{-Ikke}^{+/+}$  mice transplanted with bone marrow from  $\text{Ikke}^{+/+}$  mice, which also highlight the key contribution of Ikke expression in transformed IECs (Supplementary Fig. S10). These data highlight the contribution of Ikke in both IECs and hematopoietic cells (possibly through IL17A production through an Ikke-dependent pathway in Th17 cells) to support Wnt-driven tumor development in the intestine.

### **Ikke controls the expression of intestinal antimicrobial factors upon constitutive Wnt signaling**

GSEA analysis also identified an enrichment of intestinal antimicrobial factors among Ikke target genes in  $\beta\text{-cat}^{c.a.}$  mice (Fig. 6A). Indeed, both  $\text{Reg3}\beta/\gamma$  and  $\text{Ang4}$ , whose mRNA levels increased in transformed IECs from  $\beta\text{-cat}^{c.a.}$  mice, were downregulated upon Ikke inactivation (Fig. 6A and B). The number of Paneth cells, the major source of antimicrobial factors, was intact in  $\beta\text{-cat}^{c.a.}\text{-Ikke}^{-/-}$  mice (Supplementary Fig. S11). Yet, the number of visible antimicrobial factor releasing granules in each Paneth cell was severely decreased in intestinal crypts from  $\beta\text{-cat}^{c.a.}\text{-Ikke}^{-/-}$  mice (Supplementary Fig. S11). Therefore, Ikke deficiency interferes with Paneth cell differentiation. Of note, the goblet cell marker  $\text{Muc1}$ , whose expression increased upon constitutive Wnt signaling, was also decreased in Ikke-deficient IECs from  $\beta\text{-cat}^{c.a.}$  mice (Fig. 6B). Moreover, mRNA levels of fucosyltransferase 2 ( $\text{Fut2}$ ), an enzyme produced by innate lymphoid cells, which promotes epithelial fucosylation in the intestinal tract to protect from *Salmonella typhirium* infection (37), also severely increased upon Wnt activation but decreased in the absence of Ikke (Fig. 6B). In addition, Ikke was required for complement C3 expression in transformed IECs (Supplementary Fig. S12A). Therefore, Ikke provides an inflammatory signature in IECs upon Wnt-dependent tumorigenesis in a cell-autonomous manner.

As LPS-dependent expression of complement C3 and activation of  $\text{C/Ebp}\delta$  in mouse embryonic fibroblasts requires the transcriptional induction of Ikke through NF- $\kappa\text{B}$  (38), we assessed  $\text{C/Ebp}\delta$  expression in primary IECs from  $\text{Ikke}^{+/+}$  or  $\text{Ikke}^{-/-}$  mice subjected or not to LPS stimulation. Complement C3 expression was strongly induced by LPS at the mRNA level and Ikke deletion impaired its expression, especially after 4 and 8 hours of LPS stimulation in IECs (Supplementary Fig. S12B). Consistently,  $\text{C/Ebp}\delta$  protein levels were also decreased in Ikke-deficient IECs,

with or without LPS stimulation and in IECs from  $\beta\text{-cat}^{c.a.}\text{-Ikke}^{-/-}$  mice compared to  $\beta\text{-cat}^{c.a.}\text{-Ikke}^{+/+}$  mice (Supplementary Fig. S12C and S12D). Thus, Ikke promotes C3 expression, by regulating  $\text{C/Ebp}\delta$  levels in normal and transformed IECs.

### **Commensal bacteria promote Ikke activation in tumors from $\beta\text{-cat}^{c.a.}$ mice and the expression of inflammatory markers and antimicrobial factors**

Gut microbiota promotes tumor development in  $\text{Apc}^{+/min}$  mice (39). Moreover, commensal bacteria trigger TLR-dependent signaling pathways that converge on Ikke (19). To assess whether bacterial products trigger TLRs-dependent Ikke activation to provide the inflammatory tumor microenvironment, we subjected  $\beta\text{-cat}^{c.a.}/\text{Ikke}^{+/+}$  mice to broad-spectrum antibiotics (Abx) to deplete commensal bacteria. Bacterial counts from feces of  $\beta\text{-cat}^{c.a.}/\text{Ikke}^{+/+}$  mice validated the efficiency of antibiotics (Supplementary Fig. S13). Abx treatment prolonged mouse survival, probably by interfering with Ikke, Akt, Msk1, and Stat3 activations (Fig. 7A and B). Therefore, bacterial products trigger the Ikke-dependent activation of oncogenic pathways during Wnt-driven tumor development. We next assessed mRNA levels of pro-inflammatory cytokines and chemokines in whole duodenum from control versus Abx-treated  $\beta\text{-cat}^{c.a.}/\text{Ikke}^{+/+}$  mice. Most candidate genes whose expression was decreased in  $\beta\text{-cat}^{c.a.}/\text{Ikke}^{-/-}$  mice also showed reduced expression in Abx-treated  $\beta\text{-cat}^{c.a.}/\text{Ikke}^{+/+}$  mice (Fig. 7C). Also, similar to Ikke deficiency, the expression of multiple Paneth cells markers significantly decreased upon Abx treatment in  $\beta\text{-cat}^{c.a.}$  mice (Fig. 7D). These data identified key Ikke-dependent oncogenic pathways triggered by bacterial products that provide an inflammatory tumor microenvironment in the intestine showing constitutive Wnt signaling.

## **Discussion**

Here we define Ikke as a LPS- and IL17A-activated kinase acting upstream of multiple pathways in transformed IECs, leading to the establishment of a proinflammatory environment in two mouse models of Wnt-driven intestinal tumorigenesis. Ikke is also acting as a pro-survival kinase by limiting TNF- and caspase-8-dependent apoptosis in IECs showing constitutive Wnt signaling.

Ikke counteracts TNF-dependent cell death, similarly to the prosurvival  $\text{Ikk}\beta$  but through NF- $\kappa\text{B}$ -independent mechanisms as  $\text{I}\kappa\text{B}\alpha$  degradation and p65 phosphorylation by TNF remained intact in Ikke-deficient IECs. It is likely that the phosphorylation of multiple unknown IKK $\epsilon$  substrates will provide prosurvival signals.

(Continued.) Candidate genes up- or downregulated are illustrated in red or green, respectively. Experimental conditions are: 1 and 2, duodenal samples from  $\beta\text{-cat}^{c.a.}\text{-Ikke}^{+/+}$  mice at day 0 or 22 days after tamoxifen injection, respectively; 3 and 4, duodenal samples from  $\beta\text{-cat}^{c.a.}\text{-Ikke}^{-/-}$  mice at day 0 or 22 days after tamoxifen injection, respectively.  $n = 3$  for each genotype. B, defective chemokine production in Ikke-deficient  $\beta\text{-cat}^{c.a.}$  mice. Real-time PCR analyses were carried out with total RNAs isolated from whole mucosa of  $\beta\text{-cat}^{c.a.}/\text{Ikke}^{+/+}$  and  $\beta\text{-cat}^{c.a.}/\text{Ikke}^{-/-}$  mice, 22 days after the first tamoxifen injection. Data represent fold difference of Ct values from  $\beta\text{-cat}^{c.a.}/\text{Ikke}^{-/-}$  versus  $\beta\text{-cat}^{c.a.}/\text{Ikke}^{+/+}$  mice. Data are mean  $\pm$  SEM,  $n \geq 4$  for each genotype. C, decreased protein levels of pro-inflammatory cytokines in Ikke-deficient  $\beta\text{-cat}^{c.a.}$  mice. A chemokine protein array was conducted with protein extracts from duodenal tissues of the indicated mice, 22 days after the first tamoxifen injection. The graph shows relative fold expression. D, Ikke promotes Cxcl1 expression upon stimulation by both LPS and IL17A in transformed IECs. Total RNAs extracted from *ex vivo* organoid cultures from  $\text{Apc}^{+/min}/\text{Ikke}^{+/+}$  and  $\text{Apc}^{+/min}/\text{Ikke}^{-/-}$  mice were treated or not with the indicated ligand(s) for up to 5 hours. The abundance of Cxcl1 mRNA levels in untreated  $\text{Apc}^{+/min}/\text{Ikke}^{+/+}$  mice was set to 1 and its level in other experimental conditions were relative to that after normalization with Gapdh. Data from triplicates (means  $\pm$  standard deviations) are shown (\*\*\*,  $P < 0.001$ ; \*\*,  $P < 0.01$ ; \*,  $P < 0.05$ ). E and F, Ikke promoted the infiltration of  $\text{F4/80}^+$  (E) and  $\text{CD163}^+$  (F) myeloid cells to highly proliferating crypts in  $\beta\text{-cat}^{c.a.}$  mice 22 days after the first tamoxifen injection. Below, infiltrated  $\text{F4/80}^+$  (E) and  $\text{CD163}^+$  (F) myeloid cells were quantified as number of cells per field (per  $\text{mm}^2$ ). Data are mean  $\pm$  SEM,  $n = 3$ . G and H, decreased expression of inflammatory cell (G) and M1/M2 markers (H) in Ikke-deficient  $\beta\text{-cat}^{c.a.}$  mice. Real-time PCR analysis was carried out with total RNAs isolated from whole mucosa of  $\beta\text{-cat}^{c.a.}/\text{Ikke}^{+/+}$  and  $\beta\text{-cat}^{c.a.}/\text{Ikke}^{-/-}$  mice, 22 days after the first tamoxifen injection. Data shown represents fold difference of Ct values from  $\beta\text{-cat}^{c.a.}/\text{Ikke}^{-/-}$  versus  $\beta\text{-cat}^{c.a.}/\text{Ikke}^{+/+}$  mice. Data are mean  $\pm$  SEM,  $n \geq 4$  for each genotype.

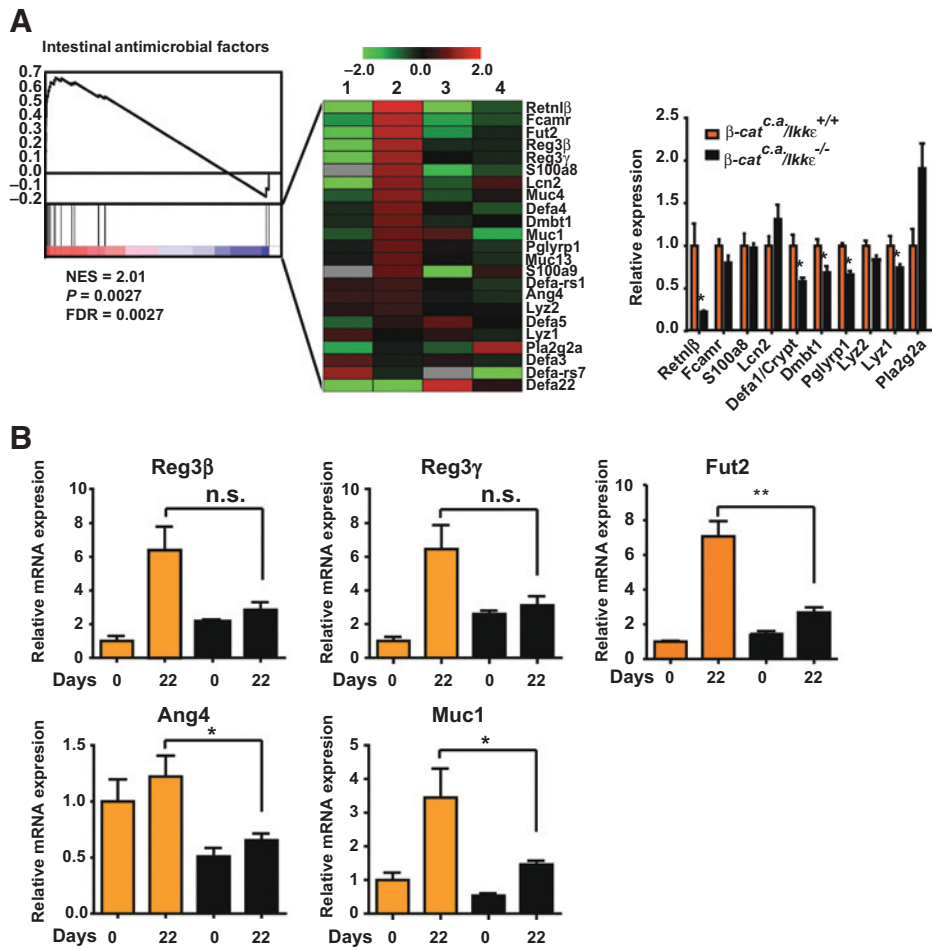


**Figure 6.** Ikke controls the expression of antimicrobial factors in transformed IECs. A, the secretion of antimicrobial factors by Paneth cells relies on Ikke in  $\beta$ -cat<sup>c.a.</sup> mice. A, GSEA of RNA-Seq expression data obtained with total RNAs from duodenal samples of  $\beta$ -cat<sup>c.a.</sup>-Ikke<sup>+/+</sup> versus  $\beta$ -cat<sup>c.a.</sup>-Ikke<sup>-/-</sup> mice is illustrated. Middle, Heatmap expression analysis from RNAseq data. Experimental conditions are: 1 and 2, duodenal samples from  $\beta$ -cat<sup>c.a.</sup>-Ikke<sup>+/+</sup> mice at day 0 or 22 days after tamoxifen injection, respectively; 3 and 4,  $\beta$ -cat<sup>c.a.</sup>-Ikke<sup>-/-</sup> mice at day 0 or 22 days after tamoxifen injection, respectively.  $n = 3$  for each genotype. Right, decreased expression of antimicrobial factors upon *Ikke* deficiency in  $\beta$ -cat<sup>c.a.</sup> mice. Real-time PCR analysis was carried out with total RNAs isolated from IECs of the indicated mice, 22 days after the first tamoxifen injection. Data from three independent experiments (means  $\pm$  standard deviations) were plotted as in Fig. 4D ( $n \geq 4$  for each genotype). B, deregulated expression of Paneth or goblet cell mRNAs (Reg3β/γ, Ang4, and Muc-1, respectively) upon constitutive Wnt signaling in duodenal samples from  $\beta$ -cat<sup>c.a.</sup>-Ikke<sup>-/-</sup> mice. Real-time PCR analysis was carried out with total RNAs isolated from IECs of the indicated mice, 0 or 22 days after the first tamoxifen injection. The abundance of each transcript in untreated  $\beta$ -cat<sup>c.a.</sup>/Ikke<sup>+/+</sup> mice was set to 1 and their level in other experimental conditions were relative to that after normalization with Gapdh. Data from three independent experiments (means  $\pm$  standard deviations) are shown ( $n \geq 4$  for each genotype). \*,  $P < 0.05$ ; \*\*,  $P < 0.01$ ; n.s., nonsignificant.

In addition to a prosurvival role, *Ikke* acts as an oncogenic kinase by stimulating the recruitment of proinflammatory cells to support Wnt-driven tumorigenesis. Our bone marrow transplantation experiments highlight a dual function for *Ikke* expression in both IECs and bone marrow-derived cells. This dual role is required to sustain a proinflammatory loop that supports tumor development, a loop initiated by *Ikke* expression in transformed IECs (Supplementary Fig. S14). Th17 cells known to produce IL17A may critically rely on *Ikke* to maintain this loop. Indeed, the key role of *Ikke* in IL1β-driven Th17 maintenance supports this hypothesis (40). Removing *Ikke* in transformed IECs or in bone marrow-derived cells disrupt this proinflammatory loop and tumor development is consequently delayed. Whether *IKKE* expression in cancer-associated fibroblasts also provide oncogen-

ic signals deserves further investigation using conditional knockout mouse models.

*Ikkβ* is another proinflammatory molecule but mechanisms by which *Ikkβ* drives Wnt-dependent tumor initiation in the intestine are partially distinct. *Ikke* is an Akt-activating kinase in *Apc*-mutated IECs whereas *Ikkβ* is not. Similarly, *Erk1/2* is regulated by *Ikke* but not by *Ikkβ*. Therefore, *Ikke* provides a proinflammatory signature in transformed IECs, at least through some specific pathways distinct from those controlled by *Ikkβ*. Previous *in vitro* studies showed that *Ikke* targets several substrates acting in NF-κB-activating cascades (23, 41). We show here that the oncogenic potential of *Ikke* in transformed IECs mainly results from its capacity to provide a tumor microenvironment rather than from enhancing pro-proliferative cascades in a cell-autonomous manner.

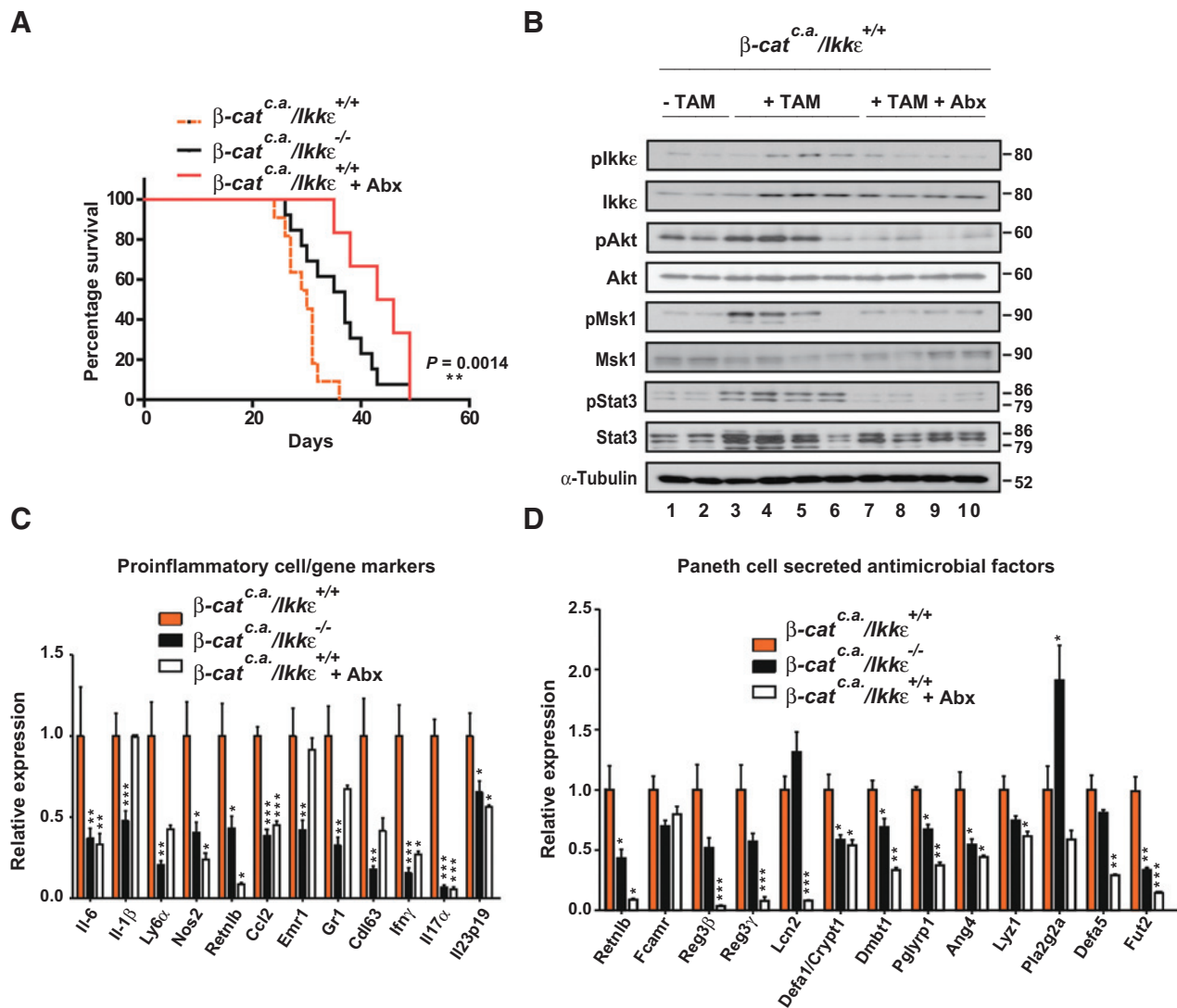


**Figure 7.**

Gut microbiome promotes *Ikke* activation and the expression of inflammatory markers and Paneth cell antimicrobial factors in tumors from  $\beta\text{-cat}^{c.a.}$  mice. A, antibiotics (Abx) treatment of  $\beta\text{-cat}^{c.a.}$  mice extends survival. A, Kaplan-Meier survival graph for  $\beta\text{-cat}^{c.a.}/Ikke^{+/+}$ ,  $\beta\text{-cat}^{c.a.}/Ikke^{-/-}$ , or  $\beta\text{-cat}^{c.a.}/Ikke^{+/+}$  mice treated with Abx [ciprofloxacin (0.5 g/L), ampicillin (1 g/L), and metronidazole (0.5 g/L)] after induction of tumorigenesis via 5 days tamoxifen injections is illustrated. Data are mean  $\pm$  SEM,  $n \geq 6$  for each genotype. B, microbiota promotes *Ikke*, Akt, Msk1, and Stat3 phosphorylations in  $\beta\text{-cat}^{c.a.}$  mice. Extracts from duodenal tissue of the indicated mice after induction of tumorigenesis were subjected to Western blotting. C and D, proinflammatory markers and antimicrobial factors whose expression is *Ikke* dependent in duodenal tissues of  $\beta\text{-cat}^{c.a.}$  mice also show lower levels of expression in Abx-treated *Ikke*-sufficient animals. Real-time PCR analysis was carried out with total RNAs isolated from whole mucosa (C) or IECs (D) of the indicated mice 22 days after the first tamoxifen injection. Data from three independent experiments (means  $\pm$  standard deviations) were plotted as in Fig. 5B ( $n \geq 4$  for each genotype).

Our data provide an *in vivo* demonstration that *Ikke* promotes Akt activation in transformed IECs. The transcriptional program induced through the *Ikke*-Akt pathway in *Apc*-mutated IECs remains unclear. One candidate could be *Retn1b*, which is upregulated in colon cancer, and protects against parasitic helminth infections by maintaining the colonic barrier function (42–44). *Retn1b* expression is induced through IL23 and Akt in intestinal goblet cells (45). Because Akt activation is *Ikke* dependent in *Apc*-mutated IECs, *Retn1b* expression may be induced through this pathway. It is likely that CREB1, whose phosphorylation occurs through Akt and Msk1 (46), contributes to the induction of numerous *Ikke* target genes. Similarly, *C/Ebp $\delta$*  is another tran-

scription factor acting downstream of *Ikke* that drives the expression of proinflammatory molecules such as complement C3.

Constitutive Stat3 activation cooperates with NF- $\kappa$ B to promote cell survival and proliferation in the intestine (14). The defective Stat3 phosphorylation profile seen upon *Ikke* inactivation results from an impaired recruitment of macrophages in the tumor stroma rather than an epithelial cell-autonomous effect of *Ikke* on Stat3. This defect causes decreased levels of Stat3-activating cytokines such as IL6 in whole duodenum from  $\beta\text{-cat}^{c.a.}/Ikke^{-/-}$  mice.

Multiple cytokines and chemokines show an *Ikke*-dependent expression in our model of Wnt-driven tumor initiation. One of

them is IL17A whose production was decreased upon Ikk $\epsilon$  deficiency. Once synthesized, IL17A can establish a positive loop by re-activating Ikk $\epsilon$  in transformed IECs. Consistently, IL17A or Ikk $\epsilon$  deficiency in *Apc<sup>+/-</sup>/min* mice similarly delays tumor development and also corrects splenomegaly (47). Therefore, signals from two distinct families of receptors, IL17RA and TLRs, converge to Ikk $\epsilon$  to promote Wnt-dependent tumor development in the intestine. Few candidates such as IL1 $\alpha$  were upregulated in duodenum of  *$\beta$ -cat<sup>ca</sup>/Ikk $\epsilon$ <sup>-/-</sup>* mice, as similarly showed in a model of arthritis (48). As IL1 $\alpha$  antagonizes the function of IL1 $\beta$ , Ikk $\epsilon$  may potentiate IL1 $\beta$  signaling by limiting IL1 $\alpha$  expression.

The recruitment of macrophages in the intestinal tumor stroma, but not their polarization, requires Ikk $\epsilon$ . This is in sharp contrast with Ikk $\alpha$  whose kinase activity is required for Wnt-driven intestinal tumor development by negatively regulating the recruitment of Interferon  $\gamma$  (IFN $\gamma$ )-producing M1-like myeloid cells (30). Therefore, Ikk $\epsilon$  establishes an inflammatory signature to promote Wnt-driven tumor development through mechanisms distinct from those implying Ikk $\alpha$  and Ikk $\beta$ .

### Disclosure of Potential Conflicts of Interest

L.C. Heukamp has ownership interest in a NEO New Oncology and reports receiving a commercial research grant from Roche, Boehringer, and MSD. No potential conflicts of interest were disclosed by the other authors.

### Authors' Contributions

**Conception and design:** S.I. Göktuna, K. Shostak, A. Ladang, A. Chariot  
**Development of methodology:** S.I. Göktuna, H.-Q. Duong, A. Ladang, P. Close, I. Klevernic, A. Florin, F. Baron, S. Rahmouni, R. Büttner, A. Chariot

### References

- Watson AJ, Collins PD. Colon cancer: a civilization disorder. *Dig Dis* 2011;29:222–8.
- Vogelstein B, Kinzler KW. Cancer genes and the pathways they control. *Nat Med* 2004;10:789–99.
- Fearon ER. Molecular genetics of colorectal cancer. *Annu Rev Pathol* 2011;6:479–507.
- Grivennikov SI, Greten FR, Karin M. Immunity, inflammation, and cancer. *Cell* 2010;140:883–99.
- Mantovani A, Allavena P, Sica A, Balkwill F. Cancer-related inflammation. *Nature* 2008;454:436–44.
- Langowski JL, Zhang X, Wu L, Mattson JD, Chen T, Smith K, et al. IL-23 promotes tumour incidence and growth. *Nature* 2006;442:461–5.
- Grivennikov SI, Wang K, Mucida D, Stewart CA, Schnabl B, Jauch D, et al. Adenoma-linked barrier defects and microbial products drive IL-23/IL-17-mediated tumour growth. *Nature* 2012;491:254–8.
- McKenzie BS, Kastelein RA, Cua DJ. Understanding the IL-23-IL-17 immune pathway. *Trends Immunol* 2006;27:17–23.
- Wang K, Kim MK, Di Caro G, Wong J, Shalpour S, Wan J, et al. Interleukin-17 receptor signaling in transformed enterocytes promotes early colorectal tumorigenesis. *Immunity* 2014;41:1052–63.
- Ghosh S, Hayden MS. New regulators of NF-kappaB in inflammation. *Nat Rev Immunol* 2008;8:837–48.
- Karin M. Nuclear factor-kappaB in cancer development and progression. *Nature* 2006;441:431–6.
- Greten FR, Eckmann L, Greten TF, Park JM, Li ZW, Egan LJ, et al. IKKbeta links inflammation and tumorigenesis in a mouse model of colitis-associated cancer. *Cell* 2004;118:285–96.
- Schwitalla S, Fingerle AA, Cammareri P, Nebelsiek T, Göktuna SI, Ziegler PK, et al. Intestinal tumorigenesis initiated by dedifferentiation and acquisition of stem-cell-like properties. *Cell* 2013;152:25–38.
- Grivennikov SI, Karin M. Dangerous liaisons: STAT3 and NF-kappaB collaboration and crosstalk in cancer. *Cytokine Growth Factor Rev* 2010;21:11–9.
- Grivennikov S, Karin E, Terzic J, Mucida D, Yu GY, Vallabhapurapu S, et al. IL-6 and Stat3 are required for survival of intestinal epithelial cells and development of colitis-associated cancer. *Cancer Cell* 2009;15:103–13.
- Bollrath J, Phesse TJ, von Burstin VA, Putoczki T, Bennecke M, Bateman T, et al. gp130-mediated Stat3 activation in enterocytes regulates cell survival and cell-cycle progression during colitis-associated tumorigenesis. *Cancer Cell* 2009;15:91–102.
- Wang K, Karin M. Common flora and intestine: a carcinogenic marriage. *Cell Logist* 2013;3:e24975.
- Fukata M, Chen A, Vamadevan AS, Cohen J, Breglio K, Krishnareddy S, et al. Toll-like receptor-4 promotes the development of colitis-associated colorectal tumors. *Gastroenterology* 2007;133:1869–81.
- Hemmi H, Takeuchi O, Sato S, Yamamoto M, Kaisho T, Sanjo H, et al. The roles of two IkappaB kinase-related kinases in lipopolysaccharide and double stranded RNA signaling and viral infection. *J Exp Med* 2004;199:1641–50.
- Fitzgerald KA, McWhirter SM, Faia KL, Rowe DC, Latz E, Golenbock DT, et al. IKKepsilon and TBK1 are essential components of the IRF3 signaling pathway. *Nat Immunol* 2003;4:491–6.
- Sharma S, tenOever BR, Grandvaux N, Zhou GP, Lin R, Hiscott J. Triggering the interferon antiviral response through an IKK-related pathway. *Science* 2003;300:1148–51.
- Shen RR, Hahn WC. Emerging roles for the non-canonical IKKs in cancer. *Oncogene* 2011;30:631–41.
- Hutti JE, Shen RR, Abbott DW, Zhou AY, Spratt KM, Asara JM, et al. Phosphorylation of the tumor suppressor CYLD by the breast cancer oncogene IKKepsilon promotes cell transformation. *Mol Cell* 2009;34:461–72.
- Renner F, Moreno R, Schmitz ML. SUMOylation-dependent localization of IKKepsilon in PML nuclear bodies is essential for protection against DNA-damage-triggered cell death. *Mol Cell* 2010;37:503–15.

**Acquisition of data (provided animals, acquired and managed patients, provided facilities, etc.):** S.I. Göktuna, T.-L. Chau, L.C. Heukamp, B. Hennuy, H.-Q. Duong, A. Ladang, P. Close, F. Olivier, G. Ehx, M. Vandereyken, S. Rahmouni, R. Büttner, F. R. Greten, A. Chariot

**Analysis and interpretation of data (e.g., statistical analysis, biostatistics, computational analysis):** S.I. Göktuna, K. Shostak, B. Hennuy, A. Ladang, G. van Loo, R. Büttner, A. Chariot

**Writing, review, and/or revision of the manuscript:** S.I. Göktuna, K. Shostak, I. Klevernic, L. Vereecke, R. Büttner, A. Chariot

**Administrative, technical, or material support (i.e., reporting or organizing data, constructing databases):** B. Hennuy, G. Ehx

**Study supervision:** A. Chariot

### Acknowledgments

The authors thank Wouters Coppieters (GIGA Transcriptomic facility, ULG, Liege, Belgium) for RNA-Seq analyses, Sophie Dubois for her help in tail injections and the GIGA Imaging and Flow Cytometry Facility.

### Grant Support

A. Chariot received grants from the Belgian National Funds for Scientific Research (F.N.R.S), TELEVIE, the Belgian Federation against cancer, the University of Liege (Concerted Research Action Program (BIO-ACET) and "Fonds Spéciaux" (C-11/03)), the "Centre Anti-Cancéreux", the "Leon Fredericq" Foundation (ULg), and from the Walloon Excellence in Life Sciences and Biotechnology (WELBIO). P. Close and A. Chariot are Research Associate and Senior Research Associate at the F.N.R.S., respectively.

The costs of publication of this article were defrayed in part by the payment of page charges. This article must therefore be hereby marked *advertisement* in accordance with 18 U.S.C. Section 1734 solely to indicate this fact.

Received June 1, 2015; revised January 21, 2016; accepted February 13, 2016; published OnlineFirst March 15, 2016.

25. Adli M, Baldwin AS. IKK-i/IKKepsilon controls constitutive, cancer cell-associated NF-kappaB activity via regulation of Ser-536 p65/RelA phosphorylation. *J Biol Chem* 2006;281:26976–84.
26. Xie X, Zhang D, Zhao B, Lu MK, You M, Condorelli G, et al. IkappaB kinase epsilon and TANK-binding kinase 1 activate AKT by direct phosphorylation. *Proc Natl Acad Sci U S A* 2011;108:6474–9.
27. Guo JP, Shu SK, Esposito NN, Coppola D, Koomen JM, Cheng JQ. IKKepsilon phosphorylation of estrogen receptor alpha Ser-167 and contribution to tamoxifen resistance in breast cancer. *J Biol Chem* 2010;285:3676–84.
28. Harada N, Tamai Y, Ishikawa T, Sauer B, Takaku K, Oshima M, et al. Intestinal polyposis in mice with a dominant stable mutation of the beta-catenin gene. *EMBO J* 1999;18:5931–42.
29. el Marjou F, Janssen KP, Chang BH, Li M, Hindie V, Chan L, et al. Tissue-specific and inducible Cre-mediated recombination in the gut epithelium. *Genesis* 2004;39:186–93.
30. Goktuna SI, Canli O, Bollrath J, Fingerle AA, Horst D, Diamanti MA, et al. IKKalpha promotes intestinal tumorigenesis by limiting recruitment of M1-like polarized myeloid cells. *Cell reports* 2014;7:1914–25.
31. Ladang A, Rapino F, Heukamp LC, Tharun L, Shostak K, Hermand D, et al. Eip3 drives Wnt-dependent tumor initiation and regeneration in the intestine. *J Exp Med* 2015;212:2057–75.
32. Shostak K, Zhang X, Hubert P, Goktuna SI, Jiang Z, Klevernic I, et al. NF-kappaB-induced KIAA1199 promotes survival through EGFR signalling. *Nat Commun* 2014;5:5232.
33. Shostak K, Patrascu F, Goktuna SI, Close P, Borgs L, Nguyen L, et al. MDM2 restrains estrogen-mediated AKT activation by promoting TBK1-dependent HPIP degradation. *Cell Death Differ* 2014;21:811–24.
34. Su LK, Kinzler KW, Vogelstein B, Preisinger AC, Moser AR, Luongo C, et al. Multiple intestinal neoplasia caused by a mutation in the murine homolog of the APC gene. *Science* 1992;256:668–70.
35. Lee JW, Wang P, Kattah MG, Youssef S, Steinman L, DeFea K, et al. Differential regulation of chemokines by IL-17 in colonic epithelial cells. *J Immunol* 2008;181:6536–45.
36. Bulek K, Liu C, Swaidani S, Wang L, Page RC, Gulen MF, et al. The inducible kinase IKK $\epsilon$  is required for IL-17-dependent signaling associated with neutrophilia and pulmonary inflammation. *Nat Immunol* 2011;12:844–52.
37. Goto Y, Obata T, Kunisawa J, Sato S, Ivanov II, Lamichhane A, et al. Innate lymphoid cells regulate intestinal epithelial cell glycosylation. *Science* 2014;345:1254009.
38. Kravchenko VV, Mathison JC, Schwamborn K, Mercurio F, Ulevitch RJ. IKK $\epsilon$ /IKKepsilon plays a key role in integrating signals induced by pro-inflammatory stimuli. *J Biol Chem* 2003;278:26612–9.
39. Li Y, Kundu P, Seow SW, de Matos CT, Aronsson L, Chin KC, et al. Gut microbiota accelerate tumor growth via c-jun and STAT3 phosphorylation in APCMin/+ mice. *Carcinogenesis* 2012;33:1231–8.
40. Gulen MF, Bulek K, Xiao H, Yu M, Gao J, Sun L, et al. Inactivation of the enzyme GSK3alpha by the kinase IKK $\epsilon$  promotes AKT-mTOR signaling pathway that mediates interleukin-1-induced Th17 cell maintenance. *Immunity* 2012;37:800–12.
41. Shen RR, Zhou AY, Kim E, Lim E, Habelhah H, Hahn WC. IkappaB kinase epsilon phosphorylates TRAF2 to promote mammary epithelial cell transformation. *Mol Cell Biol* 2012;32:4756–68.
42. Zheng LD, Tong QS, Weng MX, He J, Lv Q, Pu JR, et al. Enhanced expression of resistin-like molecule beta in human colon cancer and its clinical significance. *Dig Dis Sci* 2009;54:274–81.
43. Herbert DR, Yang JQ, Hogan SP, Groschwitz K, Khodoun M, Munitz A, et al. Intestinal epithelial cell secretion of RELM-beta protects against gastrointestinal worm infection. *J Exp Med* 2009;206:2947–57.
44. Hogan SP, Seidu L, Blanchard C, Groschwitz K, Mishra A, Karow ML, et al. Resistin-like molecule beta regulates innate colonic function: barrier integrity and inflammation susceptibility. *J Allergy Clin Immunol* 2006;118:257–68.
45. Wang ML, Keilbaugh SA, Cash-Mason T, He XC, Li L, Wu GD. Immune-mediated signaling in intestinal goblet cells via PI3-kinase- and AKT-dependent pathways. *Am J Physiol Gastrointest Liver Physiol* 2008;295:G1122–30.
46. Shaywitz AJ, Greenberg ME. CREB: a stimulus-induced transcription factor activated by a diverse array of extracellular signals. *Annu Rev Biochem* 1999;68:821–61.
47. Chae WJ, Gibson TF, Zeltermann D, Hao L, Henegariu O, Bothwell AL. Ablation of IL-17A abrogates progression of spontaneous intestinal tumorigenesis. *Proc Natl Acad Sci U S A* 2010;107:5540–4.
48. Corr M, Boyle DL, Ronacher L, Flores N, Firestein GS. Synergistic benefit in inflammatory arthritis by targeting I kappaB kinase epsilon and interferon beta. *Ann Rheum Dis* 2009;68:257–63.